

Article

Independence of Future Changes of River Runoff in Europe from the Pathway to Global Warming

Lorenzo Mentaschi ^{1,*}, Lorenzo Alfieri ¹, Francesco Dottori ¹, Carmelo Cammalleri ¹, Berny Bisselink ¹, Ad De Roo ¹ and Luc Feyen ¹

¹ European Commission, Joint Research Centre (JRC), Ispra, Italy

* Correspondence: lorenzo.mentaschi@ec.europa.eu

Abstract: The outcomes of the 2015 Paris Agreement triggered a number of climate impact assessments, such as for floods and droughts, to focus on future time frames corresponding to the years of reaching specific levels of global warming. Yet, the links between the timing of the warming levels and the corresponding greenhouse gas concentration pathways to reach them, remain poorly understood. To address this gap, we compare projected changes of annual mean, extreme high and extreme low river discharges in Europe at 1.5°C and 2°C under scenarios RCP8.5 and RCP4.5 from an ensemble of Regional Climate Model (RCM) simulations. The statistical significance of the difference between the two scenarios for both warming levels is then evaluated. Results show that in the majority of Europe (>95% of the surface area for the annual mean discharge, >98% for high and low extremes), the changes projected in the two pathways are statistically indistinguishable. These results suggest that in studies of changes at specific warming levels the projections of the two pathways can be merged into a single ensemble without major loss of information. With regard to the uncertainty of the unified ensemble, findings show that the projected changes of annual mean, extreme high and extreme low river discharge are statistically significant in large portions of Europe.

Keywords: climate change; warming levels; river runoff; extremes; emission pathway; LISFLOOD; Europe; PESETA project; climate adaptation

1. Introduction

River runoff is associated with different types of natural hazards. Extremely high flow regimes are associated with floods, a major natural hazard with considerable human and socio-economic implications [1–5]. Extreme low discharges are related with dry spells and droughts [6]. Changes in mean river discharge affect the long-term availability of water resources, necessary for the sustainability of ecosystems and agricultural activities [7,8].

The past decades saw breakthroughs in atmosphere and precipitation modelling [9–12] and in our understanding of the complex dynamics of catchment areas [13–18], as well as in our observational [19] and computational capabilities, allowing a more and more accurate investigation of large-scale, long-term issues and tendencies [3,20–22].

In view of global warming, the scientific community put a significant effort in studying how both mean and extreme river runoff values will change on the basis of climate projections, both at global scale, such as in the Coupled Model Intercomparison Project 5 (CMIP5, [23]), and at regional scale, such as in the Coordinated Regional Climate Downscaling Experiment (CORDEX, [24]), as well as to quantify the uncertainty in the projected changes [25,26]. Several past studies on future river runoff focused on specific periods in time, typically the short (2020s), medium (2050s) and long (2080s) term, in different Representative Concentration Pathway (RCP) scenarios [27]. In such studies, the projected changes clearly depend on the considered pathway in, e.g., studies related to river floods [28–32], droughts [33–35], and water resources [36–38]. It is worth mentioning the close

relationship between the trends of river runoff and the ones of forcing variables such as precipitations and temperature. The projected changes of such variables have been extensively investigated [39–41], as well as their links with extreme and mean river discharge [28,42,43].

In order to limit the impacts of climate change, the Paris Agreement [44] set the objective of limiting the global warming to well below 2°C and pursuing efforts to limit it to 1.5°C compared to pre-industrial levels. This circumstance prompted scientists to study the changes in climate and hazards at Specific Warming Levels (SWL) of 1.5 and 2°C, as well as higher levels of warming to assess the potential consequences of not achieving the targets. For example, this was assessed for floods [45–50], droughts [51,52], and for water resources [53]. The results of these studies rely on the hypothesis that the pathway to reach a certain greenhouse concentration and corresponding warming level plays a minor role in the change of the physical variables that define the hazard. The validity of such hypothesis depends on the specific nature of the variables and should be verified in each case [54]. For average and extreme temperature and precipitation there is no agreement yet on the degree of pathway-dependence [54,55]. Some studies suggest little effect of the pathway to radiative forcing and warming [56–58], while other studies report significant differences between pathways [59,60]. For other variables, such as sea level rise, the pathway has been shown to play an important role [54,61], due to the large inertia of the sea masses. Whether or not this hypothesis is valid for hydrological variables, such as high/low extreme and mean river discharges, that control riverine flood hazard, and are connected with water availability and drought onset, is yet unknown.

This topic also relates with the investigation of the uncertainty related with the emission pathway, and of its comparison with other sources of uncertainty. In this respect, this work contributes to the research on the quantification of epistemic uncertainty of modelling hydraulic variables and climate changes impacts, and to the debate on the communication of the results [62,63].

In this study we tested the pathway-dependence of future river runoff across a wide range of hydrological conditions. To this end, we produced a pan-European ensemble of river flow simulations with the hydrological model LISFLOOD [64,65] forced by a set of EURO-CORDEX [24] climate projections for the scenarios RCP8.5 and RCP4.5. The projected changes of extreme high, extreme low and annual mean discharge between the baseline present climate and warming levels of 1.5°C and 2.0°C were thereby quantified. For each of these variables the relevance of the between-pathway differences of projected change was evaluated with respect to the ensemble uncertainty. Finally, the two pathways were merged into a single ensemble, as has been previously suggested [66], and the statistical significance of the ensemble projected changes of extreme high, extreme low and annual mean runoff was thereby quantified.

2. Materials and Methods

Projections of river discharge were obtained by running the hydrological model LISFLOOD [34,35], which represents all the relevant processes related with water dynamics of the catchment areas, including surface water balance (considering the effects due to soil type, snow, frost and vegetation), ground water dynamics, river runoff and routing, water demand for anthropogenic activities. For the sake of results reproducibility [67,68] it is worth mentioning that this model is now open-source (<https://github.com/ec-jrc/lisflood-code>), and that version 2.8 was used in this study. The model was calibrated according to previous studies [69,70], and run on a domain covering Europe with a resolution of 5 km. The forcing data of temperature, precipitation, radiative forcing, wind and vapor pressure were provided by 11 bias-corrected [71,72] EURO-CORDEX Regional Climate Models (RCMs) under scenarios RCP8.5 and RCP4.5 [24,71] (Table 1). The input data of potential evapotranspiration were estimated using the LISVAP model [73] with the Penman-Monteith parameterization [74]. In this study, we used version 0.3.2 of LISVAP, which is now open-source as well (<https://github.com/ec-jrc/lisflood-lisvap>). The simulations were carried out using the present estimations of anthropogenic land use, population and anthropogenic water demand provided by

the JRC LUISA territorial modelling platform [75]. LISFOOD was run over the time horizon 1981–2100, and daily maps of river discharge (Q) were produced.

We analyzed for each river pixel how the annual means, high and low extremes of Q change from the baseline period (1981–2010) to the year of warming level ywl , i.e., the year when a SWL is reached. For each model ywl was estimated as the first year when the 30-year moving average of the GCM model's global warming time series exceeds the SWL (Table 1).

The statistics of the extremes (high and low) of Q were computed with a non-stationary approach for Extreme Value Analysis (EVA), the transformed-stationary EVA (tsEVA) [76]. This method uses discharge data over the whole time-horizon to fit the extreme value distribution, rather than data over the 30-year windows typically applied in stationary approaches. This implies that statistical fitting and extrapolation uncertainty is inherently lower, which is especially relevant for extreme events with return periods that go beyond 30 years, such as the 100-year flood. Furthermore, non-stationary techniques are better able to capture the changing statistics at different warming levels, especially in RCP8.5, where the warming continues after exceeding 2.0°C. The authors of tsEVA released an open-source MATLAB toolbox (<https://github.com/menta78/tsEva>) which was employed in this study.

The high extremes were evaluated by fitting the values of Q beyond a moving 98.5 percentile with a non-stationary Generalized Pareto Distribution (GPD), thus estimating the time-varying 100-year return level Q_{H100} and its uncertainty.

The analysis of the low extremes is to some extent complicated by the fact that Q is low-bounded to 0, and that a 0-runoff condition is met regularly in many points. This can lead to an unreliable fit of the extremes (e.g., GEV distributions with shape parameter < -0.5), and to an estimation of the return values too close/equal to zero, which would result in inaccurate projections of relative changes. To solve this problem:

- The daily time series of Q were smoothed with a monthly running mean before fitting an extreme value distribution, guaranteeing that medium term lows were considered in the fit.
- The Generalized Extreme Value (GEV) distribution was used instead of the GPD, due to the excessive proximity of the GPD threshold to 0 in many pixels.
- The pixels with fitted GEV shape parameter < -0.5 were excluded from the analysis.
- The time-varying 15-year low return level Q_{L15} was preferred to the 100-year one, due to the excessive proximity of the latter to 0 in many points.

For Q_{H100} , Q_{L15} and annual mean discharge Q_M , the relative projected change ΔQ between the baseline period (from 1981 to 2010) and the thirty years centered in ywl was computed for each scenario, RCM and warming level:

$$\Delta Q_x = \frac{Q_{x,wl} - Q_{x,bsl}}{Q_{x,bsl}}, \quad (1)$$

where the suffix x indicates one of the three considered quantities (Q_{H100} , Q_M and Q_{L15}) and bsl and wl indicate the values at the baseline and at the warming level, respectively.

For each warming level and analyzed variable the two scenarios were joined into a single 22-model ensemble, whose variance was studied, pixel by pixel, by means of a one-way, 2-group Analysis of Variance (ANOVA, e.g. [77,78]). This approach was preferred over a Welch's t-test [79], as it comes with a decomposition of the variance of the projected change, σ^2 , into its components due, respectively, to the inner (or intramodal) variability of the 2 pathways and to the difference between the pathways:

$$\sigma^2 = \sigma_{within}^2 + \sigma_{between}^2. \quad (2)$$

The importance of the between-scenario difference with respect to σ_{within} was evaluated by means of a F-test: the pathways are considered as significantly different where $p\text{-value} \leq 0.05$. The ANOVA

analysis was carried out using the python library scipy.stats version 1.4.1 (<https://docs.scipy.org/doc/scipy/reference/stats.html>).

Finally, the statistical significance of the ensemble projected change of Q_{H100} , Q_{L15} and Q_M was studied, classifying the change as significant when $|\Delta Q| > \sigma$, as proposed in a previous study on floods [32].

Table 1: Ensemble members and related years when a global warming level (1.5°C or 2°C) is surpassed under scenarios RCP8.5 and RCP4.5.

CORDEX model name	RCP8.5, year of warming level		RCP4.5, year of warming level	
	1.5°C	2°C	1.5°C	2°C
CLMcom-CCLM4-8-17_CNRM-CERFACS-CNRM-CM5	2029	2044	2035	2057
CLMcom-CCLM4-8-17_ICHEC-EC-EARTH	2026	2041	2033	2056
CLMcom-CCLM4-8-17_MPI-M-MPI-ESM-LR	2028	2044	2034	2064
DMI-HIRHAM5-ICHEC-EC-EARTH	2028	2043	2032	2054
IPSL-INERIS-WRF331F	2021	2035	2023	2042
KNMI-RACMO22E-ICHEC-EC-EARTH	2026	2042	2032	2056
SMHI-RCA4_CNRM-CERFACS-CNRM-CM5	2029	2044	2035	2057
SMHI-RCA4_ICHEC-EC-EARTH	2026	2041	2033	2056
SMHI-RCA4_IPSL-IPSL-CM5A-MR	2021	2035	2023	2042
SMHI-RCA4_MOHC-HadGEM2-ES	2018	2030	2021	2037
SMHI-RCA4_MPI-M-MPI-ESM-LR	2028	2044	2034	2064

3. Results and Discussion

The ensemble changes projected for Q_{H100} , Q_M and Q_{L15} at 1.5°C and 2.0°C are similar in the 2 pathways, with projected changes generally more intense at 2°C than at 1.5°C. Changes of Q_{H100} are in the range -15% to 32% (values at the 99th and the 1st percentiles) at 2°C. ΔQ_M values are between -19% and 36%. Q_{L15} is the variable that shows the strongest changes, ranging between <-50% to >100% (Figure 1), in line with the fact that small quantities are subject to larger relative variations.

The results of the ANOVA show that the difference between the two pathways is generally small compared with the intermodel variability for all the three variables. On average, the component of the variance $\sigma^2_{\text{between}}$ due to the differences between scenarios explains $\leq 4\%$ of the total variance for all the three considered variables ($\leq 3\%$ for high and low extremes) with slightly lower percentages at 1.5°C than at 2.0°C (Table 2). For all the three variables and for both warming levels, the intra-scenario standard deviation σ_{within} (Figure 2cd, Figure 3cd, Figure 4cd) generally has the same order of magnitude of the projected change (Figure 2ab, Figure 3ab, Figure 4ab), while σ_{between} is much smaller (Figure 2ef, Figure 3ef, Figure 4ef). The ANOVA F-test shows that the differences between scenarios are generally statistically small: at 1.5°C the p-value is larger than 0.05 in >99% of the points for the three considered variables (99.9% for Q_{H100} , 99.8% for Q_M and 99.3% for Q_{L15}). At 2.0°C these percentages decrease, but remain >95% (98% for Q_{H100} , 95.6% for Q_M and 98.2% for Q_{L15} , Table 2). We can further argue, that in this ensemble the inter-model variability is solely related with the CORDEX forcing data, while the setup of LISFLOOD is constant across all the simulations. In other words, we are not taking into account the epistemic uncertainty arising from our lack of knowledge of catchment dynamics [80,81]. Adopting different setups or even using different hydraulic models may result in increased inter-model variability.

The differences between the 2 scenarios, though generally small, point towards more intense changes in RCP8.5 for all the 3 variables, especially at 2°C. This result is driven by similar patterns of

change in precipitations (not shown). However, global studies on precipitation report a more intense increase in precipitation in scenario RCP4.5, explaining it with the fact that the concentration of aerosol is projected to decrease approximately with the same annual rate in the 2 scenarios. Consequently, when the warming level is reached, the sky is clearer of aerosol in scenario RCP4.5 [56], and this comes with a weaker shortwave radiation absorption and reflection by the atmosphere, an increased amount of shortwave radiation reaching the land surface, an increased top atmosphere radiative cooling and subsequent more intense precipitations [82]. The relevance of aerosol concentration to explaining between-pathway differences in precipitations is remarked also by other authors [59,83,84]. The results of these studies are global, therefore do not contrast with our finding of slightly more intense precipitations in scenario RCP8.5 over Europe. The projected decrease rate in aerosol concentration is not uniform across the world and across the scenarios, and the differences we found in Europe might be related with a faster depletion of black carbon and sulfur aerosols in RCP8.5 by the end of the century [85].

Overall, these results support the assumption for merging the 2 pathways into a single 22-model ensemble, for a more comprehensive estimation of extent and uncertainty of the projected changes at the two warming levels.

In the majority of Europe, the change projected by the merged ensemble is positive for the three variables (i.e., higher extremes and annual means). At 1.5°C ΔQ_{H100} , ΔQ_M and ΔQ_{L15} are positive in 83%, 94% and 77% of the pixels, respectively. At 2°C these figures slightly decrease to 80%, 89% and 73%. Accordingly, the spatial median of the projected change is positive for all the three quantities: at 1.5°C the median changes are ~8%, ~10% and ~15% for Q_{H100} , Q_M and Q_{L15} , respectively. At 2°C these figures increase up to ~10%, ~14% and ~38%.

The spatial variability of the changes differs for the three variables. For Q_{H100} the changes are positive in central Europe and in the majority of southern Europe, with the exception of Andalusia, and of part of southern Balkans and of Sicily, and are negative in the majority of Scandinavia (Figure 2ab). For Q_M the changes are positive in central and northern Europe, turning negative in Spain, and to a lesser extent in southern Italy and Greece (Figure 3ab). For Q_{L15} the differences between northern and southern Europe are the strongest, with an intense increase in extreme lows in north-eastern Europe, and an intense decrease in the south-west, the two regions separated by a slow gradient (Figure 4ab).

The statistical significance of the projected changes is different for the three variables. ΔQ_{H100} is significant in 19% and 24% of the pixels at 1.5°C and 2.0°C, respectively (Figure 2ab). Significant positive changes of ΔQ_{H100} are estimated for central Europe, covering the larger part of France, Germany, the British Isles, Benelux, Denmark, the northern/central Danube basin, western Poland and the Po River valley, while the intense changes projected in eastern Europe and in the Dniepr basin are subject to strong uncertainties. Significant negative changes of ΔQ_{H100} is found in Iceland and in part of Scandinavia.

ΔQ_M is significant in 50% and 54% of the pixels at 1.5°C and 2.0°C, respectively (Figure 3ab). The area of positive significant changes includes the whole central-north-eastern Europe and Iceland, excluding Romania and of part of Ukraine. From 1.5°C to 2.0°C a decrease of the significance of changes in the British Isles and in northern France can be observed, while the positive changes in eastern Europe, and the negative changes in Andalusia become more significant.

ΔQ_{L15} is significant in 33% and 41% of the pixels at 1.5°C and 2.0°C, respectively (Figure 4ab). A significant increase of Q_{L15} can be observed in north-eastern Europe and in Iceland, while a significant decrease is shown in the Iberian Peninsula, parts of France, Italy and the Balkans, with changes more significant at 2.0°C than at 1.5°C. The projected changes of annual means Q_M are significant on a larger area than the extremes Q_{H100} and Q_{L15} . A possible explanation for this is that the trend of Q_M follows that of the annual mean precipitation projected by the pathways. While Q_{H100} and Q_{L15} are related with extreme meteorological conditions that are inherently more challenging to identify [86].

Overall, the results on the projected changes and on their statistical significance confirm previous results. A study of 2012, carried out with an ensemble of 12 models in the emission scenario SRES A1B, reports similar patterns of change for annual mean runoff, although with stronger

negative changes in southern Europe [29]. The main difference in the projection of the 100-year return levels is a reversal of sign in the projected change in eastern Europe. Other authors, using a smaller CORDEX ensemble in scenario RCP8.5 found patterns of change similar to ours for both annual means and high extremes [32]. A further study, carried out with a different CORDEX ensemble with 3 RCP scenarios, identified patterns of change of low flow similar to the ones found in this study for QL15 [87]. Previously, a study on projected river flow regimes in 2050, carried out with the model WaterGAP3 forced by 3 GCM found patterns similar to the ones described in this contribution [88]. Other studies and reviews reporting qualitatively similar results can be mentioned [42,47,89–92].

Merging the 2 pathways into a single ensemble comes with a two-fold advantage with respect to the separate treatment of the two scenarios. On the one hand, it improves the estimation of the statistical significance of the projected change, by increasing its size from 11 to 22, and by better taking into account the pathway-related uncertainty (the emission pathways are set ex-ante as a hypothesis for the CMIP experiment, and are generally not considered as a source of uncertainty). On the other hand, a multi-pathway ensemble can simplify the discussion of the projected changes by removing from the analysis the dependency from the emission pathway, and making the results clearer and more understandable by a non-scientific public.

On the other hand, a limitation of a multi-scenario ensemble is that each emission pathway reaches similar projected changes in different time frames. Therefore, its application to studies that include evolving socio-economic scenarios (e.g. to model the impacts of climate extremes) or focusing on mitigation or adaptation would require further assumptions for the quantification of the time available for acting.

Table 2: Components of the total standard deviation for the considered ensembles expressed as percentage of explained variance.

Variable	Warming level	% explained variance		% points where $p\text{-value} \leq 0.05$
		σ^2_{within}	$\sigma^2_{between}$	
Q_{H100}	1.5°C	98.6%	1.4%	0.1%
	2.0°C	97.0%	3.0%	2.0%
Q_M	1.5°C	98.2%	1.8%	0.2%
	2.0°C	96.0%	4.0%	4.4%
Q_{L15}	1.5°C	97.2%	2.8%	0.7%
	2.0°C	97.1%	2.9%	1.2%

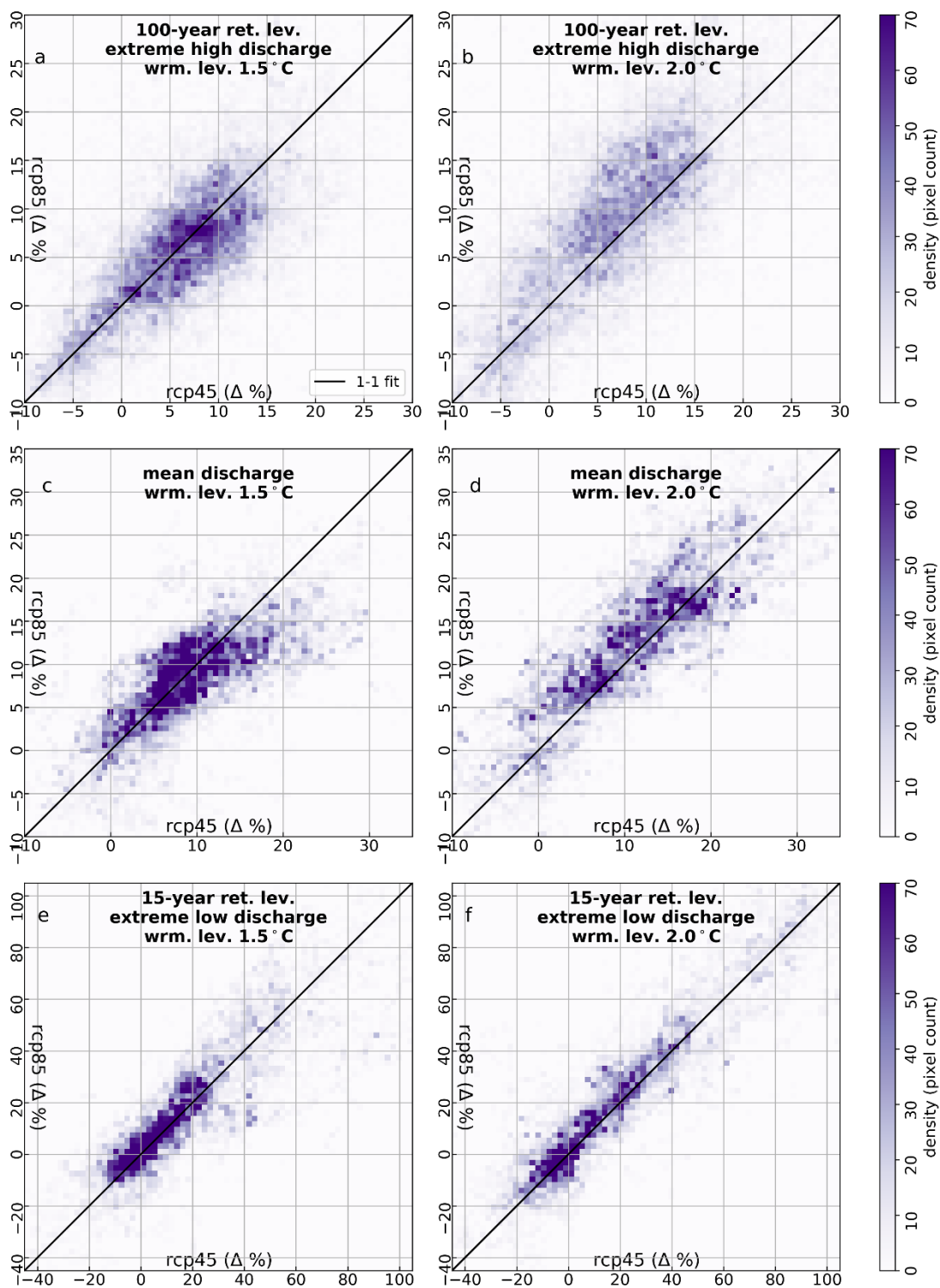


Figure 1: Projected relative changes at 1.5°C and 2.0°C warming levels. Density plots RCP8.5 vs RCP4.5 of all the pixels of the map, for high extreme (ab), mean (cd), and extreme low discharge (ef). The color of each dot represents the number domain pixels with corresponding ensemble changes in RCP8.5 and RCP4.5.

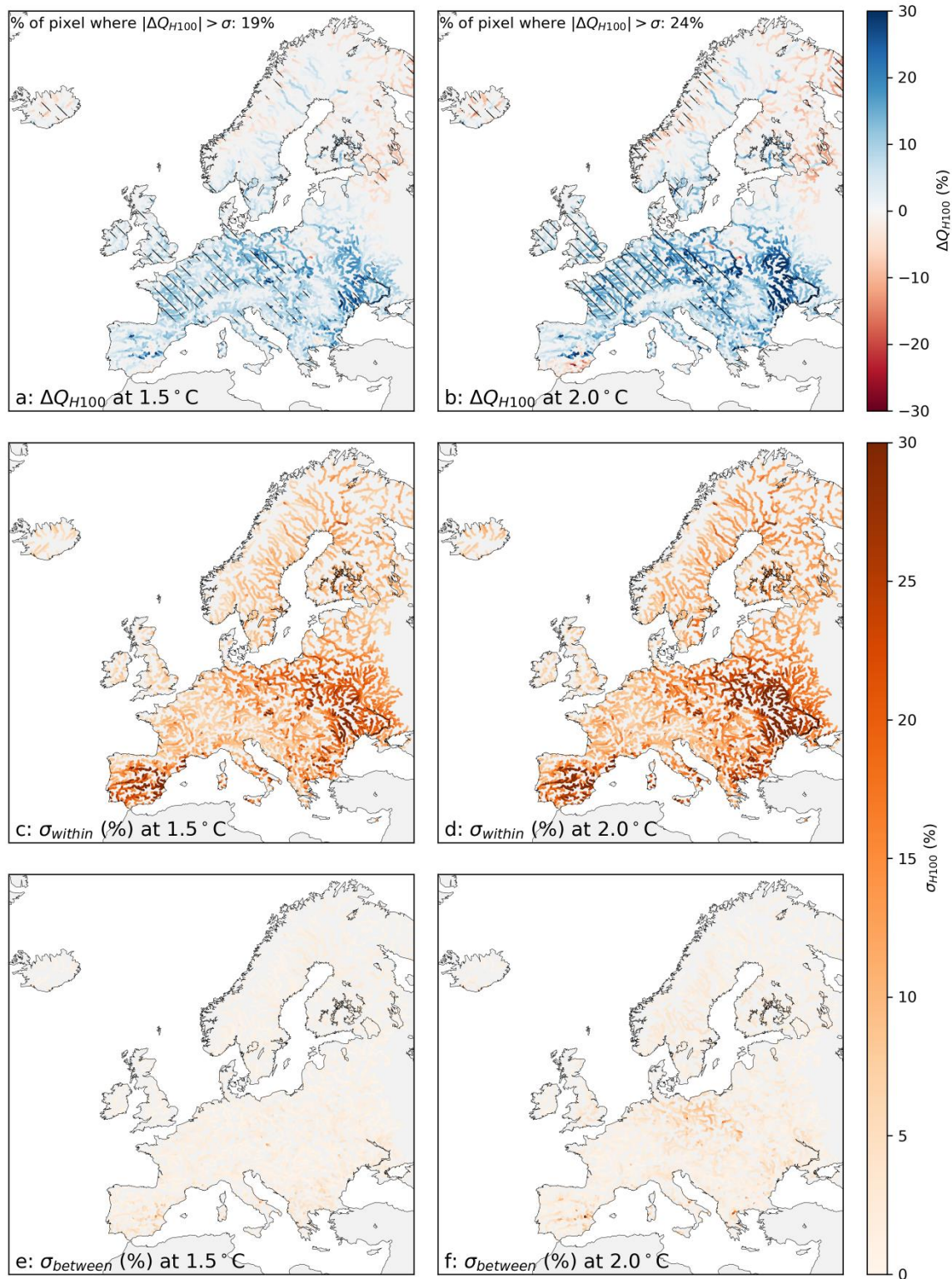


Figure 2: Projected relative change (ab), within-scenario standard deviation σ_{within} (cd), between-scenario standard deviation $\sigma_{between}$ (ef) of extreme high discharge (Q_{H100}) at warming levels 1.5°C and 2.0°C. In the hatched area in ab the ensemble projected change is statistically significant. Only network points with an upstream catchment area $>500\text{km}^2$ are shown.

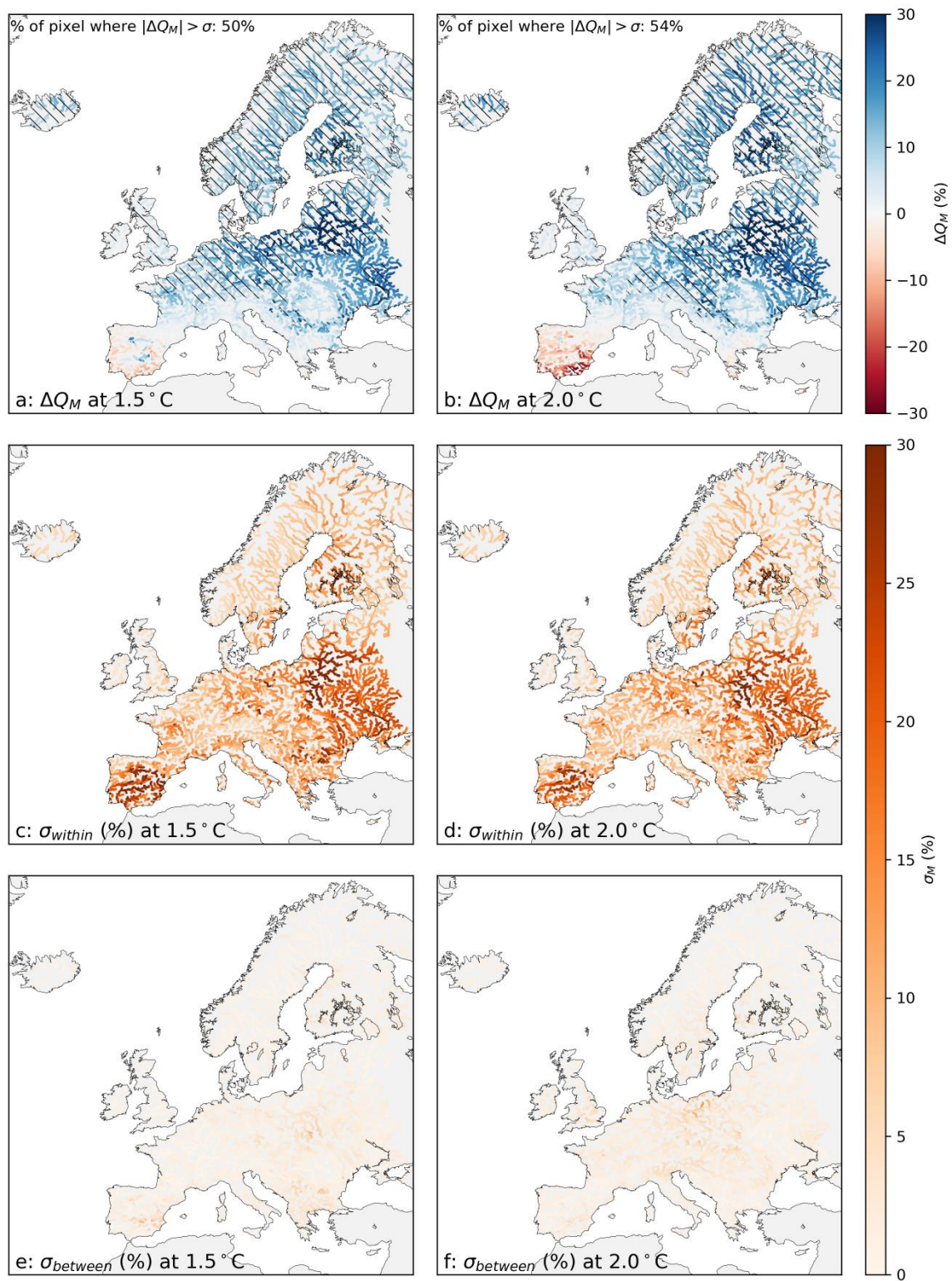


Figure 3: Same as in Figure 2 for the mean discharge (Q_M).

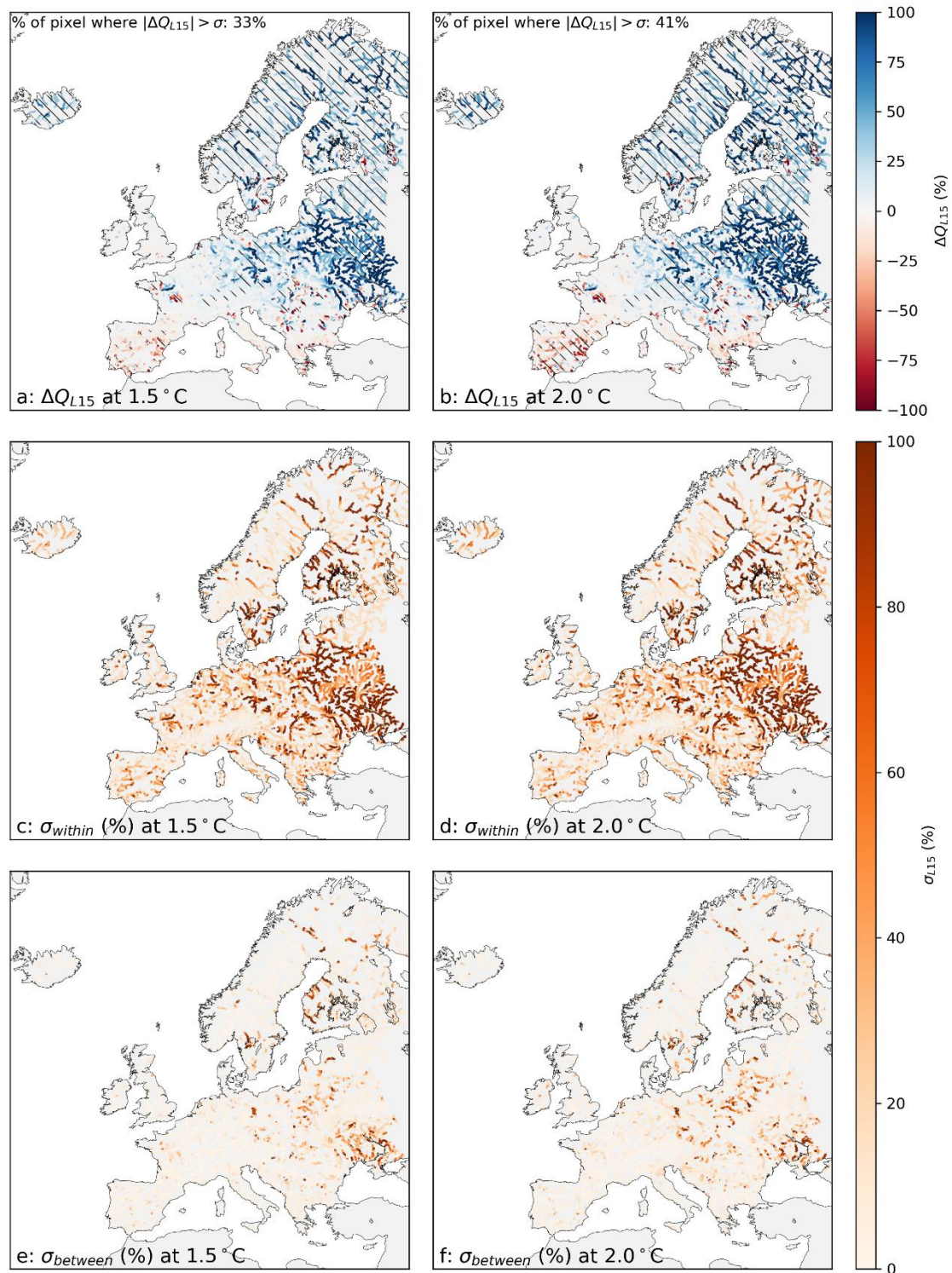


Figure 4: Same as in Figure 2 for extreme low discharge (Q_{L15}).

4. Conclusions

In this study we examined the high and low extremes and the annual means of river discharge in a changing climate at warming levels of 1.5°C and 2.0°C, under greenhouse emission scenarios RCP8.5 and RCP4.5. These three variables were chosen to provide full coverage of different regimes that have impacts on human activities, ecosystems, hazard and risk. The variance of the projected changes was studied with the ANOVA methodology, to investigate the statistical significance of the

differences between the 2 scenarios. Our results indicate that the projected changes are approximately a function of the warming level, as the between-pathway differences are generally much smaller than the within-pathway variability. The projected changes and their uncertainties were thereby studied on the joint 2-pathway, 22-model ensemble for both warming levels. The changes of high extreme runoff are found to be generally positive in central Europe, negative in Scandinavia and in Southern Europe. The other 2 variables exhibit changes mostly positive in Northern Europe and negative in Southern Europe. For all the 3 variables, the changes are generally more intense and statistically significant at 2.0°C than at 1.5°C. These results roughly agree with previous single-scenario studies.

A multi-scenario ensemble is thus found to be a viable way to provide a more comprehensive information on future changes at SWL compared to analyzing separately the different scenarios. It leads to a better evaluation of the uncertainty, not only by increasing the size of the ensemble: the future emission pathway is itself unknown, not only due to the complexity of climate dynamics and the uncertainty therein, but also due to the impossibility of predicting the commitment of the international community in mitigation efforts, or the effects of such efforts. A multi-scenario ensemble is a way to better take into account the emission pathway as a further source of uncertainty, alongside with other aspects of modelling.

Last but not least, a multi-scenario ensemble can simplify the way future climate change projections and impacts are communicated to the public, which is a relevant aspect for policy making, mitigation and adaptation [63], by shortening the discussion on the effects of different emission pathways. This can contribute to providing a clearer, more compact and summarized account of the results, better able to vehicle the information to the stakeholders and to a non-scientific public, and to favor the dissemination of knowledge.

Author Contributions: This work was conceived by Lorenzo Mentaschi and Luc Feyen. Lorenzo Mentaschi run the simulations, carried out the analysis and drafted the manuscript. Lorenzo Alfieri, Francesco Dottori, Carmelo Cammalleri, Luc Feyen and Berny Bisselink provided suggestions and manuscript review-editing. Berny Bisselink and Ad De Roo provided model input data and support.

Funding: This research was developed within the projects PESETA IV and Disaster Risk Management Knowledge Centre (DRMKC) of the JRC, European Commission.

Conflicts of Interest: The authors declare no conflict of interest.

References

1. Jongman, B.; Winsemius, H.C.; Aerts, J.C.J.H.; Coughlan de Perez, E.; van Aalst, M.K.; Kron, W.; Ward, P.J. Declining vulnerability to river floods and the global benefits of adaptation. *Proc. Natl. Acad. Sci.* **2015**, *112*, E2271–E2280.
2. Tanoue, M.; Hirabayashi, Y.; Ikeuchi, H. Global-scale river flood vulnerability in the last 50 years. *Sci. Rep.* **2016**, *6*, 36021.
3. Paprotny, D.; Sebastian, A.; Morales-Nápoles, O.; Jonkman, S.N. Trends in flood losses in Europe over the past 150 years. *Nat. Commun.* **2018**, *9*, 1985.
4. Formetta, G.; Feyen, L. Empirical evidence of declining global vulnerability to climate-related hazards. *Glob. Environ. Chang.* **2019**, *57*, 101920.
5. Kundzewicz, Z.W.; Pińskwar, I.; Brakenridge, G.R. Large floods in Europe, 1985–2009. *Hydrol. Sci. J.* **2013**, *58*, 1–7.
6. Feyen, L.; Dankers, R. Impact of global warming on streamflow drought in Europe. *J. Geophys. Res.* **2009**, *114*, D17116.

7. Calzadilla, A.; Rehdanz, K.; Betts, R.; Falloon, P.; Wiltshire, A.; Tol, R.S.J. Climate change impacts on global agriculture. *Clim. Change* **2013**, *120*, 357–374.
8. Hunink, J.; Simons, G.; Suárez-Almiñana, S.; Solera, A.; Andreu, J.; Giuliani, M.; Zamberletti, P.; Grillakis, M.; Koutroulis, A.; Tsanis, I.; et al. A Simplified Water Accounting Procedure to Assess Climate Change Impact on Water Resources for Agriculture across Different European River Basins. *Water* **2019**, *11*, 1976.
9. Kalnay, E.; Kanamitsu, M.; Kistler, R.; Collins, W.; Deaven, D.; Gandin, L.; Iredell, M.; Saha, S.; White, G.; Woollen, J.; et al. The NCEP/NCAR 40-year reanalysis project. *Bull. Am. Meteorol. Soc.* **1996**, *77*, 437–471.
10. Dee, D.P.; Uppala, S.M.; Simmons, a. J.; Berrisford, P.; Poli, P.; Kobayashi, S.; Andrae, U.; Balmaseda, M. a.; Balsamo, G.; Bauer, P.; et al. The ERA-Interim reanalysis: Configuration and performance of the data assimilation system. *Q. J. R. Meteorol. Soc.* **2011**, *137*, 553–597.
11. Hersbach, H.; Dick, L. ERA5 reanalysis is in production. *ECMWF Newsl.* **2016**, *147*, 7.
12. Saha, S.; Moorthi, S.; Pan, H.-L.; Wu, X.; Wang, J.; Nadiga, S.; Tripp, P.; Kistler, R.; Woollen, J.; Behringer, D.; et al. The {NCEP} Climate Forecast System Reanalysis. *Bull. Am. Meteorol. Soc.* **2010**, *91*, 1015–1057.
13. Arnold, J.G.; Allen, P.M.; Bernhardt, G. A comprehensive surface-groundwater flow model. *J. Hydrol.* **1993**, *142*, 47–69.
14. Allan, J.D. Landscapes and riverscapes: The influence of land use on stream ecosystems. *Annu. Rev. Ecol. Evol. Syst.* **2004**, *35*, 257–284.
15. Bates, P.D.; De Roo, A.P.J. A simple raster-based model for flood inundation simulation. *J. Hydrol.* **2000**, *236*, 54–77.
16. De Roo, A.P.J. Modelling runoff and sediment transport in catchments using GIS. *Hydrol. Process.* **1998**, *12*, 905–922.
17. Grayson, R.; Blöschl, G. *Spatial Patterns in Catchment Hydrology, Observations and Modelling*; Grayson, R., Blöschl, G., Eds.; Cambridge; Cambridge, 2001; ISBN 0-521-63316-8.
18. Brázdil, R.; Kundzewicz, Z.W.; Benito, G. Historical hydrology for studying flood risk in Europe. *Hydrol. Sci. J.* **2006**, *51*, 739–764.
19. Harris, I.; Jones, P.D.; Osborn, T.J.; Lister, D.H. Updated high-resolution grids of monthly climatic observations - the CRU TS3.10 Dataset. *Int. J. Climatol.* **2014**, *34*, 623–642.
20. Grizzetti, B.; Pistocchi, A.; Liqueste, C.; Udias, A.; Bouraoui, F.; Van De Bund, W. Human pressures and ecological status of European rivers. *Sci. Rep.* **2017**, *7*.
21. Blöschl, G.; Hall, J.; Parajka, J.; Perdigão, R.A.P.; Merz, B.; Arheimer, B.; Aronica, G.T.;

- Bilibashi, A.; Bonacci, O.; Borga, M.; et al. Changing climate shifts timing of European floods. *Science* (80-.). **2017**, *357*, 588–590.
22. Blöschl, G.; Hall, J.; Viglione, A.; Perdigão, R.A.P.; Parajka, J.; Merz, B.; Lun, D.; Arheimer, B.; Aronica, G.T.; Bilibashi, A.; et al. Changing climate both increases and decreases European river floods. *Nature* **2019**, *573*, 108–111.
 23. Taylor, K.E.; Stouffer, R.J.; Meehl, G.A. An overview of CMIP5 and the experiment design. *Bull. Am. Meteorol. Soc.* **2012**, *93*, 485–498.
 24. Jacob, D.; Petersen, J.; Eggert, B.; Alias, A.; Christensen, O.B.; Bouwer, L.M.; Braun, A.; Colette, A.; Déqué, M.; Georgievski, G.; et al. EURO-CORDEX: new high-resolution climate change projections for European impact research. *Reg. Environ. Chang.* **2014**, *14*, 563–578.
 25. Beven, K. I believe in climate change but how precautionary do we need to be in planning for the future? *Hydrol. Process.* **2011**, *25*, 1517–1520.
 26. Beven, K.; Binley, A. The future of distributed models: Model calibration and uncertainty prediction. *Hydrol. Process.* **1992**, *6*, 279–298.
 27. van Vuuren, D.P.; Edmonds, J.; Kainuma, M.; Riahi, K.; Thomson, A.; Hibbard, K.; Hurtt, G.C.; Kram, T.; Krey, V.; Lamarque, J.F.; et al. The representative concentration pathways: An overview. *Clim. Change* **2011**, *109*, 5–31.
 28. Kundzewicz, Z.W.; Luger, N.; Dankers, R.; Hirabayashi, Y.; Döll, P.; Pińskwar, I.; Dysarz, T.; Hochrainer, S.; Matczak, P. Assessing river flood risk and adaptation in Europe-review of projections for the future. *Mitig. Adapt. Strateg. Glob. Chang.* **2010**, *15*, 641–656.
 29. Rojas, R.; Feyen, L.; Bianchi, A.; Dosio, A. Assessment of future flood hazard in Europe using a large ensemble of bias-corrected regional climate simulations. *J. Geophys. Res. Atmos.* **2012**, *117*.
 30. Hirabayashi, Y.; Mahendran, R.; Koirala, S.; Konoshima, L.; Yamazaki, D.; Watanabe, S.; Kim, H.; Kanae, S. Global flood risk under climate change. *Nat. Clim. Chang.* **2013**, *3*, 816–821.
 31. Jongman, B.; Hochrainer-Stigler, S.; Feyen, L.; Aerts, J.C.J.H.; Mechler, R.; Botzen, W.J.W.; Bouwer, L.M.; Pflug, G.; Rojas, R.; Ward, P.J. Increasing stress on disaster-risk finance due to large floods. *Nat. Clim. Chang.* **2014**, *4*, 264–268.
 32. Alfieri, L.; Burek, P.; Feyen, L.; Forzieri, G. Global warming increases the frequency of river floods in Europe. *Hydrol. Earth Syst. Sci.* **2015**, *19*, 2247–2260.
 33. Prudhomme, C.; Giuntoli, I.; Robinson, E.L.; Clark, D.B.; Arnell, N.W.; Dankers, R.; Fekete, B.M.; Franssen, W.; Gerten, D.; Gosling, S.N.; et al. Hydrological droughts in the 21st century, hotspots and uncertainties from a global multimodel ensemble experiment. *Proc. Natl. Acad. Sci.* **2014**, *111*, 3262–3267.

34. Wanders, N.; Wada, Y.; Van Lanen, H.A.J. Global hydrological droughts in the 21st century under a changing hydrological regime. *Earth Syst. Dyn.* **2015**, *6*, 1–15.
35. Spinoni, J.; Vogt, J. V.; Naumann, G.; Barbosa, P.; Dosio, A. Will drought events become more frequent and severe in Europe? *Int. J. Climatol.* **2018**, *38*, 1718–1736.
36. Arnell, N.W.; Lloyd-Hughes, B. The global-scale impacts of climate change on water resources and flooding under new climate and socio-economic scenarios. *Clim. Change* **2014**, *122*, 127–140.
37. Kundzewicz, Z.W.; Piniewski, M.; Mezghani, A.; Okruszko, T.; Pińskwar, I.; Kardel, I.; Hov, Ø.; Szczesniak, M.; Szwed, M.; Benestad, R.E.; et al. Assessment of climate change and associated impact on selected sectors in Poland. *Acta Geophys.* **2018**, *66*, 1509–1523.
38. Milly, P.C.D.; Dunne, K.A.; Vecchia, A. V. Global pattern of trends in streamflow and water availability in a changing climate. *Nature* **2005**, *438*, 347–350.
39. Knutti, R.; Sedláček, J. Robustness and uncertainties in the new CMIP5 climate model projections. *Nat. Clim. Chang.* **2013**, *3*, 369–373.
40. Sillmann, J.; Kharin, V. V.; Zhang, X.; Zwiers, F.W.; Bronaugh, D. Climate extremes indices in the CMIP5 multimodel ensemble: Part 1. Model evaluation in the present climate. *J. Geophys. Res. Atmos.* **2013**, *118*, 1716–1733.
41. Kharin, V. V.; Zwiers, F.W.; Zhang, X.; Wehner, M. Changes in temperature and precipitation extremes in the CMIP5 ensemble. *Clim. Change* **2013**, *119*, 345–357.
42. Madsen, H.; Lawrence, D.; Lang, M.; Martinkova, M.; Kjeldsen, T.R. Review of trend analysis and climate change projections of extreme precipitation and floods in Europe. *J. Hydrol.* **2014**, *519*, 3634–3650.
43. Nohara, D.; Kitoh, A.; Hosaka, M.; Oki, T. Impact of climate change on river discharge projected by multimodel ensemble. *J. Hydrometeorol.* **2006**, *7*, 1076–1089.
44. United Nations Convention on Climate Change *Paris Agreement*; 2015;
45. Alfieri, L.; Bisselink, B.; Dottori, F.; Naumann, G.; de Roo, A.; Salamon, P.; Wyser, K.; Feyen, L. Global projections of river flood risk in a warmer world. *Earth's Futur.* **2017**, *5*, 171–182.
46. Alfieri, L.; Dottori, F.; Betts, R.; Salamon, P.; Feyen, L. Multi-Model Projections of River Flood Risk in Europe under Global Warming. *Climate* **2018**, *6*, 6.
47. Donnelly, C.; Greuell, W.; Andersson, J.; Gerten, D.; Pisacane, G.; Roudier, P.; Ludwig, F. Impacts of climate change on European hydrology at 1.5, 2 and 3 degrees mean global warming above preindustrial level. *Clim. Change* **2017**, *143*, 13–26.
48. Mohammed, K.; Islam, A.S.; Islam, G. tarekul; Alfieri, L.; Bala, S.K.; Khan, M.J.U. Extreme

- flows and water availability of the Brahmaputra River under 1.5 and 2 °C global warming scenarios. *Clim. Change* **2017**, *145*, 159–175.
49. Dottori, F.; Szewczyk, W.; Ciscar, J.-C.; Zhao, F.; Alfieri, L.; Hirabayashi, Y.; Bianchi, A.; Mongelli, I.; Frieler, K.; Betts, R.A.; et al. Increased human and economic losses from river flooding with anthropogenic warming. *Nat. Clim. Chang.* **2018**, *8*, 781–786.
 50. Thober, S.; Kumar, R.; Wanders, N.; Marx, A.; Pan, M.; Rakovec, O.; Samaniego, L.; Sheffield, J.; Wood, E.F.; Zink, M. Multi-model ensemble projections of European river floods and high flows at 1.5, 2, and 3 degrees global warming. *Environ. Res. Lett.* **2018**, *13*, 014003.
 51. Roudier, P.; Andersson, J.C.M.; Donnelly, C.; Feyen, L.; Greuell, W.; Ludwig, F. Projections of future floods and hydrological droughts in Europe under a +2°C global warming. *Clim. Change* **2016**, *135*, 341–355.
 52. Naumann, G.; Alfieri, L.; Wyser, K.; Mentaschi, L.; Betts, R.A.; Carrao, H.; Spinoni, J.; Vogt, J.; Feyen, L. Global Changes in Drought Conditions Under Different Levels of Warming. *Geophys. Res. Lett.* **2018**, *45*, 3285–3296.
 53. Bisselink, B.; de Roo, A.; Bernhard, J.; Gelati, E. Future Projections of Water Scarcity in the Danube River Basin Due to Land Use, Water Demand and Climate Change. *J. Environ. Geogr.* **2018**, *11*, 25–36.
 54. Zickfeld, K.; Arora, V.K.; Gillett, N.P. Is the climate response to CO₂ emissions path dependent? *Geophys. Res. Lett.* **2012**, *39*.
 55. Barring, L.; Strandberg, G. Does the projected pathway to global warming targets matter? *Environ. Res. Lett.* **2018**, *13*, 024029.
 56. Pendergrass, A.G.; Lehner, F.; Sanderson, B.M.; Xu, Y. Does extreme precipitation intensity depend on the emissions scenario? *Geophys. Res. Lett.* **2015**, *42*, 8767–8774.
 57. Maule, C.F.; Mendlik, T.; Christensen, O.B. The effect of the pathway to a two degrees warmer world on the regional temperature change of Europe. *Clim. Serv.* **2017**, *7*, 3–11.
 58. Pfeifer, S.; Rechid, D.; Reuter, M.; Viktor, E.; Jacob, D. 1.5°, 2°, and 3° global warming: visualizing European regions affected by multiple changes. *Reg. Environ. Chang.* **2019**, *19*, 1777–1786.
 59. Wang, Z.; Lin, L.; Zhang, X.; Zhang, H.; Liu, L.; Xu, Y. Scenario dependence of future changes in climate extremes under 1.5 °C and 2 °C global warming. *Sci. Rep.* **2017**, *7*, 46432.
 60. Good, P.; Booth, B.B.B.; Chadwick, R.; Hawkins, E.; Jonko, A.; Lowe, J.A. Large differences in regional precipitation change between a first and second 2 K of global warming. *Nat. Commun.* **2016**, *7*, 13667.
 61. Schaeffer, M.; Hare, W.; Rahmstorf, S.; Vermeer, M. Long-term sea-level rise implied by 1.5 °C

- and 2 °C warming levels. *Nat. Clim. Chang.* **2012**, *2*, 867–870.
62. Beven, K.J.; Aspinall, W.P.; Bates, P.D.; Borgomeo, E.; Goda, K.; Hall, J.W.; Page, T.; Phillips, J.C.; Simpson, M.; Smith, P.J.; et al. Epistemic uncertainties and natural hazard risk assessment – Part 2: What should constitute good practice? *Nat. Hazards Earth Syst. Sci.* **2018**, *18*, 2769–2783.
 63. Kundzewicz, Z.W.; Krysanova, V.; Benestad, R.E.; Hov, Ø.; Piniewski, M.; Otto, I.M. Uncertainty in climate change impacts on water resources. *Environ. Sci. Policy* **2018**, *79*, 1–8.
 64. van der Knijff, J.M.; De Roo, A.P.J. *LISFLOOD Distributed Water Balance and Flood Simulation Model*; 2008;
 65. Burek, P.; de Roo, A.; van der Knijff, J.M. *LISFLOOD - Distributed Water Balance and Flood Simulation Model - Revised User Manual*; 2013;
 66. Samaniego, L.; Thober, S.; Kumar, R.; Wanders, N.; Rakovec, O.; Pan, M.; Zink, M.; Sheffield, J.; Wood, E.F.; Marx, A. Anthropogenic warming exacerbates European soil moisture droughts. *Nat. Clim. Chang.* **2018**, *8*, 421–426.
 67. Hutton, C.; Wagener, T.; Freer, J.; Han, D.; Duffy, C.; Arheimer, B. Most computational hydrology is not reproducible, so is it really science? *Water Resour. Res.* **2016**, *52*, 7548–7555.
 68. Añel, J.A. Comment on “Most computational hydrology is not reproducible, so is it really science?” by Christopher Hutton et al. *Water Resour. Res.* **2017**, *53*, 2572–2574.
 69. Ntegeka, V.; Salamon, P.; Gomes, G.; Sint, H.; Lorini, V.; Thielen, J.; Zambrano, H. *EFAS-Meteo: A European daily high-resolution gridded meteorological data set for 1990 - 2011*; 2013;
 70. Hirpa, F.A.; Salamon, P.; Beck, H.E.; Lorini, V.; Alfieri, L.; Zsoter, E.; Dadson, S.J. Calibration of the Global Flood Awareness System (GloFAS) using daily streamflow data. *J. Hydrol.* **2018**, *566*, 595–606.
 71. Dosio, A. Projections of climate change indices of temperature and precipitation from an ensemble of bias-adjusted high-resolution EURO-CORDEX regional climate models. *J. Geophys. Res.* **2016**, *121*, 5488–5511.
 72. Casanueva, A.; Kotlarski, S.; Herrera, S.; Fernández, J.; Gutiérrez, J.M.; Boberg, F.; Colette, A.; Christensen, O.B.; Goergen, K.; Jacob, D.; et al. Daily precipitation statistics in a EURO-CORDEX RCM ensemble: added value of raw and bias-corrected high-resolution simulations. *Clim. Dyn.* **2016**, *47*, 719–737.
 73. Burek, P.; van der Knijff, J.M.; Ntegeka, V. *LISVAP Evaporation Pre-Processor for the LISFLOOD Water Balance and Flood Simulation Model*; 2013;
 74. Beven, K. A sensitivity analysis of the Penman-Monteith actual evapotranspiration estimates. *J. Hydrol.* **1979**, *44*, 169–190.

75. Batista e Silva, F.; Gallego, J.; Lavalle, C. A high-resolution population grid map for Europe. *J. Maps* **2013**, *9*, 16–28.
76. Mentaschi, L.; Vousdoukas, M.; Voukouvalas, E.; Sartini, L.; Feyen, L.; Besio, G.; Alfieri, L. The transformed-stationary approach: a generic and simplified methodology for non-stationary extreme value analysis. *Hydrol. Earth Syst. Sci.* **2016**, *20*, 3527–3547.
77. Girden, E.R. *ANOVA: Repeated measures.*; 1992; ISBN 0-8039-4257-5 (Paperback).
78. Blanca, M.J.; Alarcón, R.; Bendayan, R.; Arnau, J.; Bono, R. Non-normal data: Is ANOVA still a valid option? *Psicothema* **2017**, *29*, 552–557.
79. Welch, B.L. THE GENERALIZATION OF ‘STUDENT’S’ PROBLEM WHEN SEVERAL DIFFERENT POPULATION VARLANCES ARE INVOLVED. *Biometrika* **1947**, *34*, 28–35.
80. Beven, K. Facets of uncertainty: epistemic uncertainty, non-stationarity, likelihood, hypothesis testing, and communication. *Hydrol. Sci. J.* **2016**, *61*, 1652–1665.
81. Beven, K.; Westerberg, I. On red herrings and real herrings: disinformation and information in hydrological inference. *Hydrol. Process.* **2011**, *25*, 1676–1680.
82. Pendergrass, A.G.; Hartmann, D.L. The atmospheric energy constraint on global-mean precipitation change. *J. Clim.* **2014**, *27*, 757–768.
83. Lin, L.; Wang, Z.; Xu, Y.; Fu, Q. Sensitivity of precipitation extremes to radiative forcing of greenhouse gases and aerosols. *Geophys. Res. Lett.* **2016**, *43*, 9860–9868.
84. Lin, L.; Wang, Z.; Xu, Y.; Fu, Q.; Dong, W. Larger Sensitivity of Precipitation Extremes to Aerosol Than Greenhouse Gas Forcing in CMIP5 Models. *J. Geophys. Res. Atmos.* **2018**, *123*, 8062–8073.
85. Lamarque, J.F.; Kyle, P.P.; Meinshausen, M.; Riahi, K.; Smith, S.J.; van Vuuren, D.P.; Conley, A.J.; Vitt, F. Global and regional evolution of short-lived radiatively-active gases and aerosols in the Representative Concentration Pathways. *Clim. Change* **2011**.
86. Tabari, H.; Hosseinzadehtalaei, P.; AghaKouchak, A.; Willems, P. Latitudinal heterogeneity and hotspots of uncertainty in projected extreme precipitation. *Environ. Res. Lett.* **2019**, *14*, 124032.
87. Roudier, P.; Andersson, J.C.M.; Donnelly, C.; Feyen, L.; Greuell, W.; Ludwig, F. Projections of future floods and hydrological droughts in Europe under a +2°C global warming. *Clim. Change* **2016**, *135*, 341–355.
88. Schneider, C.; Laizé, C.L.R.; Acreman, M.C.; Flörke, M. How will climate change modify river flow regimes in Europe? *Hydrol. Earth Syst. Sci.* **2013**, *17*, 325–339.
89. García-Ruiz, J.M.; López-Moreno, I.I.; Vicente-Serrano, S.M.; Lasanta-Martínez, T.; Beguería,

- S. Mediterranean water resources in a global change scenario. *Earth-Science Rev.* 2011, *105*, 121–139.
90. Arnell, N.W. The effect of climate change on hydrological regimes in Europe: A continental perspective. *Glob. Environ. Chang.* **1999**, *9*, 5–23.
91. Gampe, D.; Nikulin, G.; Ludwig, R. Using an ensemble of regional climate models to assess climate change impacts on water scarcity in European river basins. *Sci. Total Environ.* **2016**, *573*, 1503–1518.
92. Dankers, R.; Feyen, L. Climate change impact on flood hazard in Europe: An assessment based on high-resolution climate simulations. *J. Geophys. Res. Atmos.* **2008**, *113*.